New developments accelerating catalyst research

Computational chemistry with fundamental reaction kinetics streamlines innovative catalytic discoveries

J. P. BOITIAUX, H. CAUFFRIEZ and P.-Y. LE GOFF, Axens, Rueil-Malmaison, France

Catalytic reforming accounts for a large share of the world's gasoline production; it is the most important source of aromatics for the petrochemical industry. In addition, reforming is also a major source of refinery hydrogen—whose demand is growing rapidly due to escalating hydrotreating needs.

Catalysts play the dominant role in the reforming process. Although the state of the art has advanced remarkably, even the smallest improvements in catalyst selectivity, activity and stability can have significant impacts on refinery economics. The incentive for catalyst improvements is high.

Catalyst improvement discovery and development can result from simple laboratory work to more extensive and sophisticated techniques. The maturity of reforming catalysts and their highly sophisticated nature mean that improvement through simple experimentation has given way to more complex methods. Extensive experimental programs can be used to test all conceivable possibilities individually, but acquisition, validation and interpretation of massive amounts of acquired data may be unwieldy.

Factorial experimentation, which requires careful planning, optimization and statistical treatment, can be used to reduce costs and save time. Each method has its advantages and disadvantages. Alternatively, computational chemistry, beginning with the Arrhenius equation and using *ab initio* calculations, is on the rise to guide catalyst improvement discovery. For some particular cases, this technique can provide a swifter, more direct route to the desired results.

Ab initio calculations stemming from fundamental kinetics, the Hartree-Fock Molecular Orbital Theory and Density Functional Theory[1] were used to significantly improve a commercial reforming catalyst that exhibited satisfactory performance. The designating objective was to increase selectivity by modifying the carrier and metallic cluster. By applying these computational tools, the desired results were achieved and confirmed quickly and directly with minimum experimentation.

Selectivity increase through carrier modifications. A catalyst improves the rates of the reactions producing desirable products while reducing the rates of the side reactions that produce undesirable products. In reforming, dehydrocyclization reactions are desirable; they produce aromatics and hydrogen. In contrast, the undesirable side reactions—hydrogenolysis and hydrocracking—are suppressed/avoided. These reactions produce low-value gases and consume hydrogen. The starting point is the Arrhenius equation:

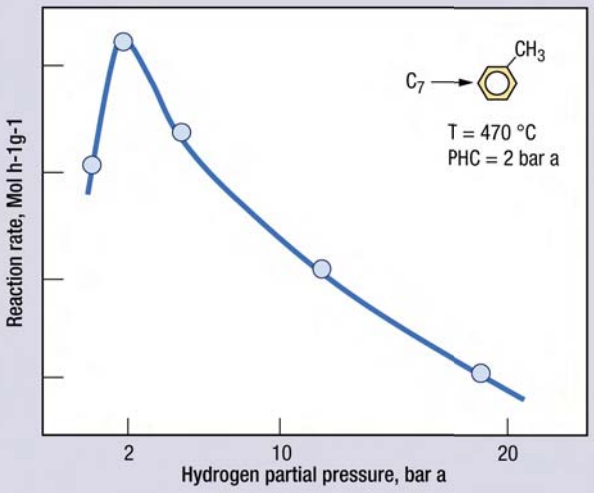

FIG. 1 Effect of hydrogen partial pressure on heptane aromatization reaction rate.

$$\Re = \mathrm{K}f(Pi, Pj, \ldots) = \mathrm{A}e^{\frac{-E_a}{\mathrm{R}\times T}} f(Pi, Pj, \ldots) \quad (1)$$

where $\Re$ = Reaction rate
K = Rate constant, J/mol
A = Pre-exponential factor
E_a = Apparent activation energy, J
R = Gas constant (8.314 J/(mol*K)
T = Absolute temperature (K)
$f(Pi, Pj, \ldots)$ = Function of the partial pressures (pp) of the reaction components.

Fig. 1 shows the characteristic reaction-rate volcano curve obtained experimentally for heptane dehydro-cyclization to toluene using a platinum catalyst on a γ alumina carrier.[2] The chloride content at the end of each test ranged from 0.9 wt% to 1.1 wt%.

The hydrogenolysis reaction is also characterized by a volcano curve. Modifying the catalyst support can change the relationship between the two curves with the goal of maximizing the ratio of the two relative reaction rates to favor dehydrocyclization.

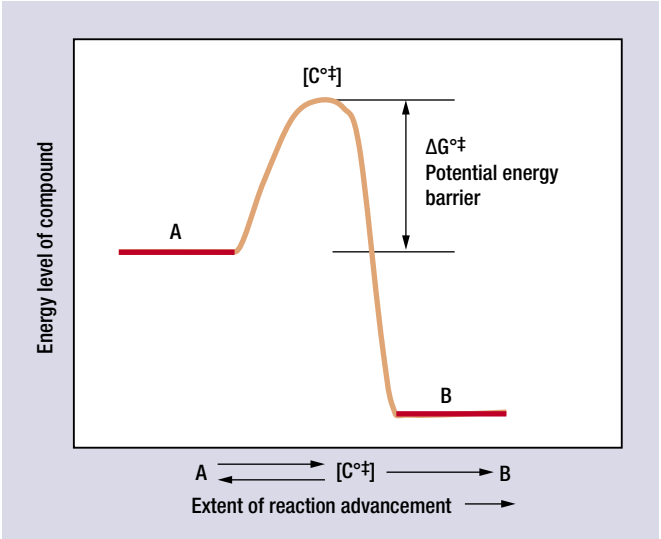

FIG. 2 Energy profile along a reaction path.

Activated complex theory.[3] This theory provides a more detailed description of the pre-exponential factor, A, and apparent energy of activation, E_a. In this theory, the reaction rate is equal to the rate of formation of activated complexes ([C‡]) forming a compound, B, by passing beyond the potential energy barrier as illustrated in Fig. 2.

An intrinsic rate constant, k′, is associated with the reaction rate and defined by the equation:

$$k' = \left(\frac{kT}{h}\right) e^{\frac{-\Delta G^{\circ\ddagger}}{RT}} \quad (2)$$

where k = Boltzmann constant
h = Planck constant
$\Delta G^{\circ\ddagger}$ = Gibbs free energy of activation = $\Delta H^{\circ\ddagger} - T\Delta S^{\circ\ddagger}$

Derivation of a more detailed kinetics equation.[4] If the dehydrocyclization of heptane to toluene were the only parameter to be considered, the operating point for Fig. 1 would be selected at 2 bars for the maximum reaction rate. However, under typical reforming catalyst operating conditions, the hydrogen partial pressure must be sufficiently high to control coke formation. Focusing on the operating point further down on the right-hand slope of the volcano curve, Eq. 3 is valid for the dehydrocyclization and hydrogenolysis reactions:

$$\Re = k'\left(k_{HC}P_{HC}\right)^{\alpha}\left(k_{H_2}P_{H_2}\right)^{\beta} \quad (3)$$

where k' = Intrinsic rate constant
P_{HC} and P_{H_2} = Partial pressures of hydrocarbon and hydrogen
k_{HC} and k_{H_2} = Adsorption constants for hydrocarbon and hydrogen
α and β = Hydrocarbon and hydrogen reaction orders, both negative.

An adsorption constant is described by the expression:

$$-RT\ln k_{HC} = \Delta H - T\Delta S \rightarrow kHC = e^{\frac{\Delta S}{R}} e^{-\frac{\Delta H}{RT}} \quad (4)$$

Substitution of Eqs. 4 and 2 into Eq. 3 yields:

$$\Re = \frac{kT}{h}\left(P^{\beta}{}_{H_2}P^{\alpha}{}_{HC}\right) e^{\left(\frac{\Delta S^{\circ\ddagger}+\beta\Delta S_{H_2}+\alpha\Delta S_{HC}}{R}\right)} e^{\left(-\frac{\Delta H^{\circ\ddagger}+\beta\Delta H_{H_2}+\alpha\Delta H_{HC}}{RT}\right)} \quad (5)$$

Factors in Eq. 1 are identified with corresponding terms in Eq. 5 providing a more detailed description of the pre-exponential factor and apparent activation energy:

$$A = \left(\frac{kT}{h}\right) e^{\frac{\Delta S^{\circ\ddagger}+\beta\Delta S_{H_2}+\alpha\Delta S_{HC}}{R}}$$

$$E_A = \Delta H^{\circ\ddagger} + \beta\Delta H_{H_2} + \alpha\Delta H_{HC} \quad (6)$$

Eq. 6 indicates that the pre-exponential factor is essentially dependent on the entropy variations of the reactants and that the activation energy is dependent on adsorption enthalpy variations. For reactant entropies, variations are negative during the adsorption step because adsorption on the catalyst surface results in a more organized structure than in the gas phase. The effect is similar during the subsequent formation of the activated complex.

The phenomenon of adsorption on the catalyst surface is exothermic, and the ΔH values are negative: generally, the stronger the adsorption, the more negative the values of ΔS and ΔH.

For heterogeneous catalysts, changes in apparent activation energies due to catalyst modifications always lead to compensatory effects between the apparent activation energy and the pre-exponential factor.[5,6] Consequently, the variations in entropy due to carrier modifications need to be taken into account together with enthalpy variations.

Application to paraffin conversion.
The logarithm of Eq. 5 yields:

$$\ln\Re = \ln\left[\frac{kT}{h}\left(P^{\beta}{}_{H_2} * P^{\alpha}{}_{HC}\right)\right] + \left(\frac{\Delta S^{\circ\ddagger}+\beta\Delta S_{H_2}+\alpha\Delta S_{HC}}{R}\right) - \left(\frac{\Delta H^{\circ\ddagger}+\beta\Delta H_{H_2}+\alpha\Delta H_{HC}}{RT}\right) \quad (7)$$

To analyze the impact of acidity variation on reaction rates, the derivative of Eq. 7 is taken with respect to an acidity estimator, χ. χ can be, for example, the isoelectric point of the catalyst. Values of the isoelectric point can vary based on a function of the amount of promoter on a continuous basis. The mathematical expression of the derivative is expressed in Eq. 8:

$$\frac{d}{d\chi}\ln\Re = \frac{d}{d\chi}\left\{\ln\left[\frac{kT}{h}\left(P^{\beta}{}_{H_2} * P^{\alpha}{}_{HC}\right)\right]\right\} - \frac{1}{RT}\left[\frac{d\Delta G^{\circ\ddagger}}{d\chi} + \frac{d\left(\beta * \Delta G_{H_2}\right)}{d\chi} + \frac{d\left(\alpha * \Delta G_{HC}\right)}{d\chi}\right] \quad (8)$$

Some simplifications can be made to Eq. 7. The first part of the equation can be neglected because the gas phase composition is essentially constant, and therefore, the derivative is zero. Furthermore, $\Delta G^{\circ\ddagger}$ is the energy variation when adsorbed molecules become activated complexes. This phenomenon is linked to con-

formation rearrangements, and thus, is mostly independent of the carrier acidity; therefore, $\frac{d\Delta G^{\circ\ddagger}}{d\chi}$ can be neglected.

In addition, experimental evidence shows that there is almost no variation in the hydrogen order of reaction (β) as a function of carrier acidity.[7,8] Thus, for example, the derivative of $\beta\Delta H_{H_2}$ with respect to acidity becomes:

$$\frac{d\left(\beta\Delta G_{H_2}\right)}{d\chi} = \beta\frac{d\Delta G_{H_2}}{d\chi} + \Delta G_{H_2}\frac{d\beta}{d\chi} = \beta\frac{d\Delta G_{H_2}}{d\chi}$$

Moreover, a reduction of the carrier acidity induces an increase of the hydrogen and hydrocarbon interaction with the metal. This effect is larger for hydrogen adsorption than for hydrocarbon adsorption.[4,9,10]

Taking into account the above remarks, Eq. 8 can be reduced to:

$$\frac{d\ln\Re}{d\chi} = -\frac{\beta}{RT}\frac{d\Delta G_{H_2}}{d\chi} \quad (9)$$

As $\frac{d\Delta G_{H_2}}{d\chi}$ is positive when the catalyst acidity is reduced, and if β is negative, a reduction in carrier acidity induces a reduction in the reaction rate.

Experimental evidence has shown that the hydrogen orders of reaction, β, are negative for hydrogenolysis and for dehydrocyclization.[10] Fortunately, β is more negative for hydrogenolysis than for dehydrocyclization.[11] As a consequence, an increase in hydrogen adsorption, linked to reduced acidity, would promote dehydrocyclization over hydrogenolysis.

Evidence of the hydrogen adsorption modification. Tables 1 and 2 provide evidence that, by modifying catalyst formulation, it is possible to change the interaction between hydrogen and platinum.

For catalysts A, B and C (Table 1[12]), a γ_c alumina was used as the carrier material. The catalysts were prepared with two successive impregnations: first, an aqueous solution of potassium carbonate, then a solution of platinum acetylacetonate dissolved in toluene.

The comparison of potassium contents, acidities and hydrogen desorption temperatures for the three catalysts are summarized in Table 1. The data suggest that, as potassium content increases (reduced acidity), higher desorption temperatures (i.e., higher hydrogen adsorption strengths) result.

The experimental data are in agreement with *ab initio* calculations[4] and can be explained by modification of the platinum electronic configuration through electron transfer from the carrier to the metallic cluster.

Two catalysts, D and E, were prepared by impregnating H_2PtCl_6 on γ_c alumina[4,7] (Table 2). No evidence of acidity difference was evoked in the referenced papers, but the thermal desorption of hydrogen strongly suggests different hydrogen adsorption energies for the two catalysts.

To set the operating point on the right-hand slopes of the volcano curves for hydrogenolysis, paraffin aromatization and hydrocracking, the test conditions were selected as follows:

Hydrogen partial pressure: 10 bar-a (144 psia)
Normal heptane partial pressure: 2.2 bar-a (32 psia)
Reactor inlet temperature: 470°C (878°F)

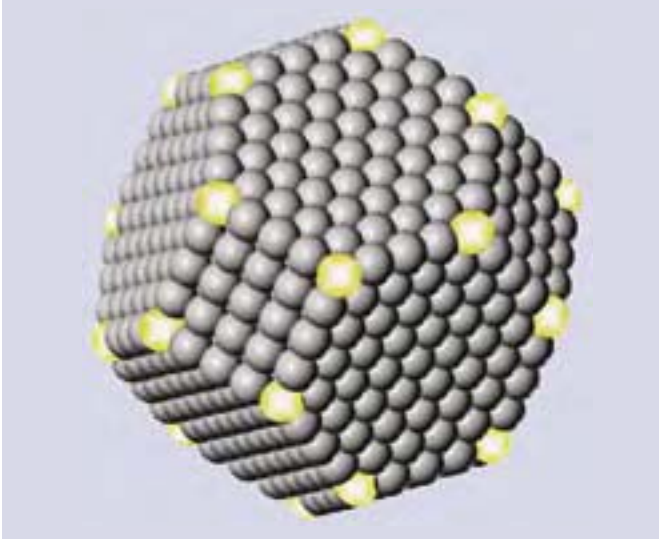

FIG. 3 Platinum metallic cluster showing promoter atoms.

As expected by the reaction rate equation, the sample exhibiting the stronger adsorption of hydrogen promotes paraffin aromatization over hydrogenolysis and hydrocracking. Indeed, the ratio of the paraffin aromatization rate to either the rate of hydrogenolysis or hydrocracking is higher.

The data show that modifying the carrier acidity for a given metal formulation can change the catalyst selectivity. For example, in the case of paraffin dehydrocyclization, in agreement with *ab initio* calculations, reducing catalyst acidity improves paraffin aromatization.[4]

Selectivity increases via metallic cluster changes. Catalyst selectivity, i.e., the extent that desired reactions are favored over undesired reactions, can be improved by alloying platinum with promoters, such as tin or copper, on specific sites in the structure of a metallic cluster (Fig. 3). For example, the hydrogenolysis reaction requires the formation of carbene-like compounds,[14] which are composed of more than a single bond between carbon and a metal. This favors selective adsorption at corner and edge sites. Therefore, any reduction or suppression of these sites leads to an increase in selectivity.

Results from *ab initio* calculations proved that tin is positioned most often at corner sites; therefore, as hydrogenolysis is hindered by tin, the reformate selectivity is improved.[15] Experimentation has shown the impact of alloying a metal with tin on catalyst selectivity.

Experimental evidence.[16] The alcohol-to-ketone dehydrogenation reaction over a nickel catalyst illustrates the effect of geometry by promoter addition on metal selectivity as only the metal function is involved (Fig. 4).

The main reaction produces ketone, but some side reactions occur due to the hydrogenolysis activity of nickel. To determine the extent of hydrogenolysis as a function of catalyst tin content, hydrogen purity was analyzed. The results (Fig. 5) show that hydrogen purity improves significantly with increasing tin content, accompanied by a comparatively small change in molar conversion.

Application to reforming catalyst optimization. The targeted products in reforming are hydrogen, aromatics for petrochemicals and reformate for refining. A good catalyst should therefore avoid fuel gas and liquefied petroleum gas (LPG) production.

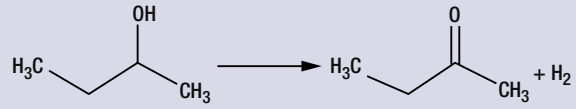

FIG. 4 The alcohol-to-ketone dehydrogenation reaction over a Ni catalyst.

TABLE 1. Hydrogen desorption temperatures for various platinum-based catalysts

Catalyst	Potassium, wt%	Acidity	Hydrogen desorption temperature, K
A	0.00	+++	495
B	0.25	++	535
C	2.90	+	655

TABLE 2. Hydrogen desorption temperature for various platinum-based catalysts

Catalyst	D	E
Hydrogen desorption temperature, °C	250	280
Aromatization rate/hydrogenolysis rate	14.3	19.4
Aromatization rate/hydrocracking rate	17.1	25.1

TABLE 3. 1-Butene-to-isobutene isomerization activity

	90°C	150°C
500 support only	Base	Base
600 support only	Base * 0.73	Base * 0.80

LPG production. LPG production is mainly the consequence of acidic site catalyzed cracking. Even on neutral catalyst, some LPG can be detected, but the amount is very small. Thus, fine-tuning the alumina acidity is required, particularly the chloride content.

Fuel-gas production. Methane and ethane formation are thought to be results of acidic mechanisms going through primary and secondary carbocations, which are not promoted under reforming operating conditions. These energy-related considerations are the basis of the conclusion that methane and ethane are more probably produced through other mechanisms occurring on the metal phase. Unlike LPG, reducing fuel gas production through acidity adjustment is a consequence of the carrier's influence on metal electronic density.

Catalyst optimization for selectivity improvement.

During the development of advanced semi-regenerative reforming catalysts, the objective was to reduce the hydrogenolysis activity of the metal function and reduce acidic site cracking. The quality improvement between the two catalysts was obtained by modifying carrier acidity.

To evaluate carrier acidity, experiments were conducted on the isomerization of butene to isobutene on a platinum-rhenium (Pt-Re) reforming catalyst (500 carrier) and an advanced nanometer-technology Pt-Re reforming catalyst (600 carrier) as shown in Table 3. At temperatures of 90°C (194°F) and 150°C (302°F), the latter catalyst exhibited lower skeletal isomerization rates.

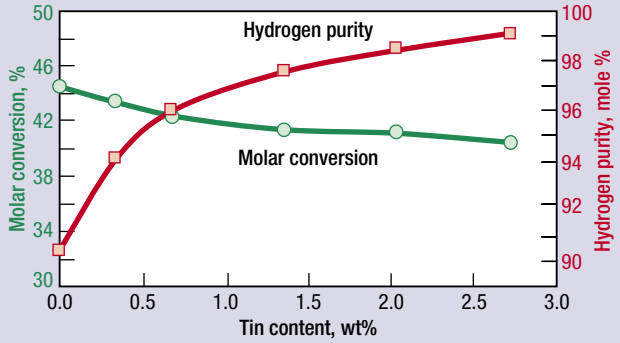

FIG. 5 Impact of tin on suppressing hydrogenolysis.

TABLE 4. Summary of performance benefits

Yields, wt%	Standard PtRe	Nanometer technology, 600
H_2	Base	Base + 0.06
C_1+C_2	Base	Base – 0.2
C_3+C_4	Base	Base – 0.4
C_5+	Base	Base + 0.6
Pressure = 11 barg, RONC = 98, LHSV = 3/h, H_2/HC = 2.5, PNA = 58/28/14 wt%		

TABLE 5. Commercial performance benefits of optimized and non-optimized catalysts

Yields, wt%	Non-optimized manufacturing	Manufacturing process
H_2	Base – 0.1	Base
C_1+C_2	Base + 0.4	Base
C_3+C_4	Base + 0.5	Base
C_5+	Base – 0.8	Base
Pressure = 20 barg, RONC = 98, WHSV = 3/h, H_2/HC = 3, PNA = 54/32/15 wt%		

TABLE 6. Benefit obtained with optimized Pt/Sn interaction

Catalyst	Activity, °C	C_5+ , wt%	Coke, wt%
A	Base	Base	Base
B	Base +5°C	Base + 0.7	Base * 0.75
Pressure = 3 barg , RONC = 104 , WHSV = 3/h, H_2/HC = 3, PNA = 54/32/15 wt%			

Consequently, and as shown in Table 4, the selectivity of Pt-Re 600 is greater than that of Pt-Re 500.

Another parameter critical to obtaining higher performance is the scale-up of experimental results to a commercial catalyst formulation. Optimizing the catalyst formulation at lab scale is not enough. For example, if the promoter distribution is not optimized, the catalyst performance is often significantly reduced.

The impact of the promoter distribution on selectivity (yield improvement) is illustrated in Table 5. The standard deviation for the promoter distribution of the non-optimized catalyst is 40%, while that for the current manufacturing processes is 13%. Consequently, the catalytic performance for the non-optimized catalyst is considerably below that of the commercial product.

The goal is not only to focus on the total composition, but also to provide a nanoscale control of the homogeneity of the

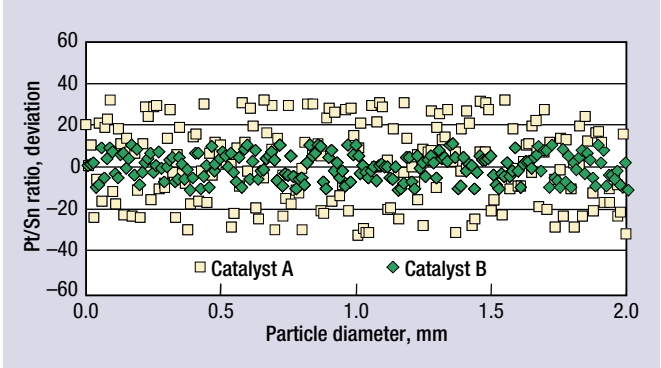

FIG. 6 Pt/Sn deviation versus average Pt/Sn ratio along the particle diameter.

metallic phase and promoter dispersion in large-scale production. For example, highly sophisticated preparation methods for controlling the surface reaction of the tin precursor on supported platinum crystals were developed. Local compositions have been measured using electronic microprobe analysis and have been complemented by scanning transmission electron microscopy. The tighter control of the Pt/Sn ratio throughout the catalyst particle diameter for catalyst B compared with catalyst A is illustrated in Fig. 6.

CCR catalyst. As shown in Table 6, an improvement in platinum-tin (Pt-Sn) metallic phase homogeneity (A compared to B) leads to a substantial enhancement in catalytic performance evaluated at 3 barg pressure.

Despite the current high performance of commercial reforming catalysts, improved reforming catalysts have been developed by modifying carrier acidity and by enhancing the metal-alloy interactions. The approach taken to arrive at a better commercial catalyst differs from conventional approaches that require extensive data acquisition and interpretation efforts.

Currently, detailed analyses of the fundamental kinetic reactions, the use of *ab initio* simulations and better understanding of metallic cluster formulations are used to accelerate development of optimized reforming catalysts. Consequently, it has been possible to substantially reduce in size and duration, experimental programs to confirm reforming catalyst selectivity improvements.

An important final step remains the scale-up from laboratory to commercial manufacturing process while achieving the same high level of catalytic performance within the limitations of the manufacturing constraints. **HP**

LITERATURE CITED

[1] Kohanoff, J., *Electronic Structure Calculations for Solids and Molecules,* Cambridge University Press, 2006.
[2] Le Goff, P.-Y., F. Le Peltier, B. Domergue and J.-F. Joly, European Refining Technology Conference, Paris, November 2002.
[3] Moore, W. J., *Physical Chemistry,* Longman, 1974.
[4] Oudenhuijzen, M. K., Thesis, Utrecht University, 2002.
[5] Lynggaard, H., et al., *Prog. Surf. Sci,* 2004, 77, pp. 71–137.
[6] Andreasem, A., et al., *Journal of Physical Chemistry,* B. 2005, pp. 3,340–3,344, 109.
[7] Alvarez Herrera, C., Thesis, Université Poitiers, 1977.
[8] Abolhamd, G., Thesis, Université Paris 6, 1980.
[9] Ramaker, D. E., et al., *Journal of Catalysis,* 2001, pp. 7–17, 203.
[10] Koningsberger, D. C., et al., *Journal of Catalysis,* 2003, pp. 178–191, 216.
[11] Imelik, B., *Catalyse par les Métaux,* CNRS Editions, 1984.
[12] Frank, J. P., *Catalyse par les Métaux,* CNRS Editions, 1984, pp. 419, 425.
[13] Rochefort, A., Thesis, Université Paris 6, 1992.
[14] Roisin, E., Thesis, Lyon, 2006.
[15] Humblot, F., Thesis, Lyon – 1, 1995.
[16] Bournonville, J. P., et al., US Patent 4,389,673, April 19, 1983.
[17] Atkins, P. W. , *Physical Chemistry,* Oxford University Press, 1994.

Jean-Paul Boitiaux is Axens' director of development and Industrialization and is responsible for the development and quality control of Axens' corporate products. He began his career with a US company in catalyst sales and technical assistance and then came to IFP where, over a period of 15 years, he held positions as IFP research engineer, project manager and director of research for catalysis. From IFP, he joined Procatalyse where he was technical director. He came to Axens in 2001 when he was named to his current position. Dr. Boitiaux received his engineering degree from Ecole de Chimie de Strasbourg and his PhD in catalysis from Université de Paris V.

Hervé Cauffriez is IFP project manager for catalytic reforming and paraffins isomerization. He started his professional career as a research engineer at IFP and developed several catalysts for various refining processes. Dr. Cauffriez holds an engineering degree from the Ecole de Chimie de Mulhouse and a PhD from the Université de Haute Alsace.

Pierre-Yves Le Goff is Axens' senior technical manager for reforming and aromizing replacement catalysts. He is also project leader in the development of the reforming catalysts in conjunction with IFP. He started his professional career as a research engineer at Rhodia where he worked mainly in the field of inorganic chemistry, specializing in catalyst support design. He was also involved in process development. Dr. Le Goff holds an engineering degree from the Ecole de Chimie de Mulhouse, an MBA from Université de la Sorbonne in Paris, and a PhD from the Université de Haute Alsace.